Title

Species Differences in the Geometry of the Anterior Segment Differentially Affect Anterior Chamber Cell Scoring Systems in Laboratory Animals

Journal

Journal of Ocular Pharmacology and Therapeutics, 32(1)

ISSN

1080-7683

Authors

Thomasy, Sara M
Eaton, J Seth
Timberlake, Matthew J
et al.

Publication Date

2016

DOI

10.1089/jop.2015.0071

Peer reviewed

JOURNAL OF OCULAR PHARMACOLOGY AND THERAPEUTICS
Volume 32, Number 1, 2016

DOI: 10.1089/jop.2015.0071

Species Differences in the Geometry of the Anterior Segment Differentially Affect Anterior Chamber Cell Scoring Systems in Laboratory Animals

Sara M. Thomasy,[1,2] J. Seth Eaton,[1,2] Matthew J. Timberlake,[3] Paul E. Miller,[2,4] Steven Matsumoto,[5] and Christopher J. Murphy[1,2,6]

Abstract

Purpose: To determine the impact of anterior segment geometry on ocular scoring systems quantifying anterior chamber (AC) cells in humans and 7 common laboratory species.
Methods: Using normative anterior segment dimensions and novel geometric formulae, ocular section volumes measured by 3 scoring systems; Standardization of Uveitis Nomenclature (SUN), Ocular Services On Demand (OSOD), and OSOD–modified SUN were calculated for each species, respectively. Calculated volumes were applied to each system's AC cell scoring scheme to determine comparative cell density (cells/mm^3). Cell density values for all laboratory species were normalized to human values and conversion factors derived to create modified scoring schemes, facilitating interspecies comparison with each system, respectively.
Results: Differences in anterior segment geometry resulted in marked differences in optical section volume measured. Volumes were smaller in rodents than dogs and cats, but represented a comparatively larger percentage of AC volume. AC cell density (cells/mm^3) varied between species. Using the SUN and OSOD–modified SUN systems, values in the pig, dog, and cat underestimated human values; values in rodents overestimated human values. Modified normalized scoring systems presented here account for species-related anterior segment geometry and facilitate both intra- and interspecies analysis, as well as translational comparison.
Conclusions: Employment of modified AC cell scoring systems that account for species-specific differences in anterior segment anatomy would harmonize findings across species and may be more predictive for determining ocular toxicological consequences in ocular drug and device development programs.

Introduction

Biomicroscopic observation of anterior chamber (AC) cell is a common diagnostic feature of anterior segment inflammation in humans and laboratory species.[1–7] Furthermore, slit lamp-facilitated scoring of AC cell permits clinicians and investigators to characterize patterns of inflammation, assess severity, and to longitudinally monitor disease progression and response to therapy. Accuracy and precision of such scoring schemes, however, are likely to be influenced by a number of factors, including the semiquantitative grades for AC cell count, as well as slit lamp parameters such as beam height and width, angle of illumination, light intensity, and magnification.

The Standardization of the Uveitis Nomenclature (SUN) system is the most widely utilized system for scoring AC cell in physician-based ophthalmology, adapted from criteria developed by the International Uveitis Study Group.[1] The slit lamp technique for SUN scoring is simple to perform, using a table-mounted slit lamp with 25× magnification and an optical section measuring 1-mm height ×1-mm width.[1] By establishing a scoring standard and specifications for slit lamp settings, the SUN system enhances the comparability of clinical data between individuals and across databases and may provide a more comprehensive understanding of uveitic disease in human patients.

The SUN system and other slit lamp-based scoring systems have become standards for preclinical ocular drug/device

[1]Department of Surgical and Radiological Sciences, School of Veterinary Medicine, University of California, Davis, Davis, California.
[2]Ocular Services on Demand (OSOD), Madison, Wisconsin.
[3]Sacramento, California.
[4]Department of Surgical Sciences, School of Veterinary Medicine, University of Wisconsin, Madison, Madison, Wisconsin.
[5]Department of Nonclinical and Translational Sciences, Allergan, Irvine, California.
[6]Department of Ophthalmology and Vision Science, School of Medicine, University of California, Davis, Davis, California.

safety programs[8] and are used to evaluate the AC cell in laboratory species.[2,9,10] Between species and even among different strains, a varied spectrum of ocular inflammatory responses may be observed in response to a given insult and may differ considerably from those in humans. Currently, no scoring systems account for species-specific anatomic and geometric parameters, including AC depth, posterior corneal radius of curvature, corneal diameter, and/or anterior lens curvature. Acknowledging that such factors may heavily influence AC scoring in a given species, lack of consideration may bias data evaluation and influence the toxicologic or translational significance assigned to the AC cell score (or other findings involving the anterior segment). As the Food and Drug Administration currently requires an investigational ocular drug or device to be evaluated in at least 2 species, use of a scoring metric that can be applied across all species would not only improve comparison of preclinical data but also may enhance translatability to humans.

There are additional aspects of the SUN system not ideally suited to evaluation of the anterior segment in laboratory species. Table-mounted slit lamp examinations are often impractical in animals, requiring additional time, technical support, and often sedation or general anesthesia. In addition, systems that do not specify an angle of slit beam illumination (like SUN) permit variability in the AC volume sampled by an optical section. This may impact consistency and repeatability of AC sampling, particularly in unanesthetized animals.

To address these limitations and allow assessment of a range of laboratory species, Ocular Services On Demand (OSOD, Madison, WI) utilizes a unique scoring system and grading scheme, as well as a modified version intended to mimic the SUN system and permit use of the SUN grading scheme (Table 1). Both systems utilize a hand-held slit lamp (eg, Kowa SL-15™), permitting assessment of the anterior segment in nonanesthetized or anesthetized laboratory species. The technique for the OSOD system and OSOD–modified SUN system, which utilizes altered beam dimensions to mimic the $\sim 3.5\,mm^3$ volume optical section in human patients created using the SUN system, is described in Table 2.

Hypothetically, consideration of comparative ocular anatomy will reveal dramatic differences in AC cell scoring between species, regardless of the system and scheme being employed. Furthermore, mathematical characterization and correction for such variations will facilitate comparison between species and potentially permit better translatability to the human condition. Presented is a detailed comparative analysis, evaluating the effect of anterior segment geometry on AC scoring in common laboratory species and humans using the SUN, OSOD, and OSOD–modified SUN systems.

Methods

A comparative analysis of all 3 systems for evaluation of AC cell (SUN, OSOD, and OSOD–modified SUN) was performed. Analysis of the system cited by Krzystolik et al.[11] (Tables 1 and 2) was not performed due to lack of specificity regarding slit lamp settings and beam dimensions. Values for ocular biometric or volumetric parameters in sexually mature humans and 7 relevant laboratory species (cynomolgus macaque [*Macaca fascicularis*)], cat [*Felis catus*], dog [*Canis familiaris*], rabbit [*Oryctolagus cuniculus*], pig [*Sus domesticus*], rat [*Rattus norvegicus*], and mouse [*Mus musculus*]) were derived from published or approximated data collected by OSOD members.

The optical section volumes (mm^3) examined by each system were calculated for all aforementioned species, using both *simplified* and *complex* analytical calculations. Simplified calculations were performed by multiplying slit lamp beam area and AC depth. This value was also multiplied by a 1.15 correction factor to account for a 30° angle light source incidence. For the OSOD and OSOD–modified SUN systems, actual vertical corneal diameter (VCD) was substituted in species with a VCD less than 10 mm.

To account for species-specific differences in corneal and lens curvatures, complex geometric formulae (Fig. 1) were derived to provide a more accurate estimate of optical section volumes used in the OSOD and OSOD–modified SUN systems. Complex calculations also accounted for 30° angle light source incidence. Again, in species with VCD less than 10 mm, the actual VCD value was substituted for slit beam height.

The percentage of AC volume sampled by each system was determined by using data from simplified or complex calculations. Also using the values derived from these calculations, the SUN, OSOD, or OSOD–modified SUN grading schemes for AC cells were applied to all aforementioned species to calculate cell density (cells/mm^3 of optical section volume) for each, respectively. To directly compare AC cell density across species, modified scoring systems yielding normalized cell density values across all species were then derived by multiplying the human values for AC cell density (cells/mm^3) by the optical section volumes for each species using the SUN, OSOD, or OSOD–modified SUN grading schemes, respectively. A conversion factor for each species was determined by dividing the human AC cell density by the AC cell density for each species using the SUN, OSOD, or OSOD–modified SUN grading schemes.

Additional analytical comparisons were performed to evaluate the effect of species-specific anatomy on optical section and AC volumes. To demonstrate the effect of anterior

Table 1. Description of Grading Schemes for Commonly Used Scoring Systems to Quantify AC Cell

	Grading scheme (cells in field)					
Scoring system	*0*	*Trace (0.5+)*	*1+*	*2+*	*3+*	*4+*
SUN[1]	0	1–5	6–15	16–25	26–50	>50
OSOD	0	1–5	6–25	26–50	51–100	>100
OSOD–modified SUN	0	1–5	6–15	16–25	26–50	>50
Krzystolik et al.[11]	0	—	<10	10–20	21–30	TNTC

AC, anterior chamber; SUN, standardization of uveitis nomenclature; OSOD, Ocular Services On Demand; TNTC, too numerous to count.

Table 2. Approximate Human AC Volume Examined and Slit Lamp Specifications for Commonly Used Scoring Systems to Quantify AC Cell

Scoring system	Approximate examined volume (mm^3)[a]	Slit lamp Specifications			
		Width	Height	Angle (°)	Magnification
SUN[1]	3.50	1	1	NS[b]	25×
OSOD	7	0.2	14	30–45	16×
OSOD–modified SUN	3.50	0.1	10	30	16×
Krzystolik et al.[11]	ND	NS	2	NS	High

[a]AC depth used was 3.03 mm.[6]
[b]Calculated at 30°.
ND, not determined; NS, not specified.

segment anatomical features (corneal diameter and curvature, iris position/thickness, and anterior lens curvature) on optical section volume, optical coherence tomography (OCT) images of the anterior segments of 6 species (human, nonhuman primate, rat, mouse, dog, and rabbit; $n = 1$ for each species) were analyzed. A computer-aided drafting (CAD) program (SketchUp Make™, Trimble™, Sunnyvale, CA) was used to manually trace and measure the cross-sectional areas of the AC and iris leaflets (when applicable), providing an area measurement of each traced region.

All animal procedures were approved by the Institutional Animal Care and Use Committee at the University of California, Davis (Davis, CA) and Covance (Madison, WI), and were conducted in accordance with the ARVO Statement for Use of Animals in Ophthalmic and Vision Research.

Results

Values calculating the approximate human AC volume (mm^3) examined by common AC cell scoring systems are presented in Table 2. Values for selected ocular biometric and volumetric parameters (axial globe length, corneal diameter, posterior corneal curvature, AC depth, AC volume, anterior lens curvature, and lens diameter) that are important for calculating optical section volumes are presented for the human, cynomolgus monkey, cat, dog, rabbit, pig, rat, and mouse; marked differences in values for these parameters are observed between some species (Table 3). CAD-analyzed anterior segment OCT images representing 6 species (human, cynomolgus monkey, rat, mouse, dog, and rabbit) are also presented in Fig. 2. The majority of the AC area is shown in orange, the iris (when reducing effective AC area) in green, and increase in AC area adjacent to the peripheral anterior lens in blue. Spatial analysis of these individual images reveals that anterior lens curvature increases the AC area in the mouse by 35%, the rat by 6%, the dog by 30%, and the rabbit by 19%.

Optical section volume (mm^3) calculations and percentage of AC volume calculations using simplified and complex (Fig. 1) formulae for all 3 scoring systems are presented in Tables 4 and 5, respectively. Regardless of the formulae and/or scoring system utilized, optical section volumes are much smaller in rats and mice, but represent a larger percentage of AC volume compared to other species. By contrast, cats and dogs have the largest optical section volumes sampled, but represent a smaller percentage of AC volume in comparison to other species.

The AC cell grading schemes for each system (Table 1) were applied to optical section volume calculations to determine AC cell density (cells/mm^3) for each species and are presented in Tables 6 and 7. For the OSOD scoring system, note that the simplified calculations underestimate AC cell density by 25%, 40%, 25%, 25%, and 15% in the human, cynomolgus monkey, cat, mouse and rabbit, respectively, and overestimate the AC cell density by 50% and 30% in the pig and rat, respectively (Table 6). For humans, cynomolgus monkeys, and rabbits, the SUN and OSOD–modified SUN grading schemes both yield similar cell densities with less than 12% difference between the 3 species for each individual scheme (Table 7). However, the SUN and OSOD–modified SUN grading schemes yield cell densities measuring between 77% and 88% of the human values in pigs and 58% and 71% of the human values in dogs and cats, while rats and mice have much higher values compared to humans at 442%–2,390% (Table 7). The SUN grading scheme yields less variability between species in comparison to the OSOD–modified SUN grading scheme (Table 7).

A modified scoring scheme and conversion factor for each species were calculated for the SUN, OSOD–modified SUN, and OSOD grading systems (Table 8). Scoring schemes for cynomolgus monkeys and rabbits are the most similar to humans and require the smallest conversion factors in comparison to other species for all 3 scoring systems. Modified scoring schemes and conversion factors substantially differed in species with comparatively larger AC volumes, such as the cat, dog, and pig, or species with substantially smaller AC volumes, such as the rat or mouse, compared to the human. In general, the size of the conversion factor required for each grading scheme was SUN<OSOD–modified SUN<OSOD.

Discussion

Identification and quantification of the AC cell is a critical element of assessing ocular inflammation in human patients and in laboratory animals used in preclinical drug safety investigations. The results of this analysis demonstrate the dramatic influence of anterior segment anatomy and geometry on optical section volume and semiquantitative AC cell count when using standard scoring systems in common laboratory species. As the majority of preclinical drug safety investigations utilize more than 1 nonhuman species, awareness of these comparative differences is critical in the application and accurate interpretation of any ocular scoring system and/or AC cell grading scheme. Furthermore, parameters, such as beam

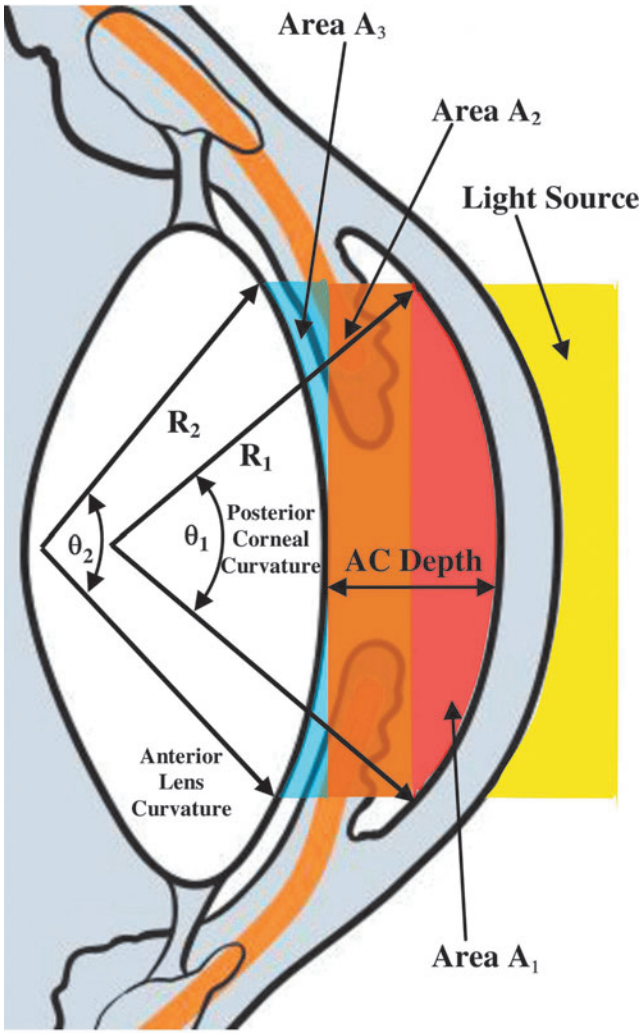

FIG. 1. A simple estimate of the optical section volume can be calculated using the height and width of the slit beam and the anterior chamber (AC) depth. To develop a more accurate calculation of optical section volume within the AC, the following geometric formulae were derived to account for the curvature of the cornea and lens, the angle of the light source, and the effective length of the light source intersecting the AC. The standard and modified Standardization of Uveitis Nomenclature [SUN] using the slit beam height and width specified in Table 2 for each scoring system. The formulae used for calculating optical section volume calculations for SUN scoring systems. These formulae provide values for Ocular Services On Demand measurements, both are also below. Color images available online at www.liebertpub.com/jop

$$\theta = 2 * sin^{-1} \frac{Half\ of\ Slit\ Lamp\ Beam\ Height\ (mm)}{R\ (Corneal\ Curvature)\ (mm)} \tag{1}$$

Area created by the angle in formula 1:

$$A_0 = \frac{\theta}{360} * \pi * R^2 \tag{2}$$

Area of circle segment, shown in *red*:

$$A_1 = A_{\theta_1} - \frac{R^2 * \sin\theta}{2} \tag{3}$$

Area of the slit lamp through the AC, shown in *orange*:

$$A_2 = Slit\ Lamp\ Beam\ Height\ (10\ or\ 14\ mm) * \left(AC\ Depth\ (in\ mm) - R\left(1 - cos\frac{\theta}{2}\right)\right) \tag{4}$$

Remaining area of the slit lamp through the AC, shown in *blue*:

$$A_3 = \mathrm{R}_2\left(1 - cos\frac{\theta_2}{2}\right) * Slit\ Lamp\ Beam\ Height\ (10\ or\ 14\ mm) - \left(A_{\theta_2} - \frac{R^2 * \sin\ \theta}{2}\right) \tag{5}$$

Volume of Slit Lamp Beam Penetration in mm^3 (Divide by 1000 for ml):

$$V = Slit\ Lamp\ Beam\ Width\ (0.1\ or\ 0.2mm) * (A_1 + A_2 + A_3) \tag{6}$$

As comparison, Table 4 also includes values for the SUN criterion:

$$V = 1mm * 1mm * AC\ Depth\ (mm)$$

Table 3. Relative Comparison of Selected Ocular Parameters of Relevant Laboratory Animal Species

Species	*Axial globe length (mm)*	*Corneal diameter (mm)*	*Posterior corneal curvature (mm)*	*AC depth (mm)*	*AC volume (ml)*	*Anterior lens curvature (mm)*	*Lens diameter (mm)*
Human	25.1[13]	H: 11.81 V: 11.26[14]	6.5[15]	3.03[16]	0.17[17]	10.15[18]	9.5[19]
Cynomolgus	17.92[20]	H: 9.8[21]	5.12[20]	3.24[20]	0.101[22]	10.34[20]	7.5[23]
Cat	22.3[24]	H: 16.5 V: 16.2[25]	7.89[24]	4.52[24]	0.82[26]	6.0[27]	9.0[27]
Dog	20.8[28]	H: 13–17 V: 12–16[27]	8.0[29]	4.29[28]	0.77[30]	6.2[27]	10.92[27]
Rabbit	15.12[31]	H: 13.4 V: 13.0[31]	6.89[31]	2.9[32]	0.28[32]	7.1[33]	11[32]
Pig	23.9[34]	H: 14.3 V: 12.0[34]	8.95[29]	3.45[29]	0.26[35]	7.47[29]	11.1[36]
Rat	5.98[37]	5.1 (Est)	2.96[38]	0.71[38]	0.015[39]	2.54[38]	5.1[40]
Mouse	3.38[41]	3.15 (Est)	1.46[38]	0.45[38]	0.007[42]	1.25[38]	1.9[43]

Values are approximates and derived from published values using a variety of techniques. Calculations based on published values for schematic eyes and data collected by OSOD members. Values in the literature vary by technique, age, strain, and study.
Est, estimated.

area and AC depth, can be used to derive simple calculations of optical section volume, but the results of such calculations do not adequately account for all features of anterior segment anatomy.

When comparing optical section volume using complex geometric formulae that incorporate parameters such as corneal curvature and anterior lens curvature, this analysis demonstrated that simplified calculations may over- or underestimate optical section volume depending on the species evaluated (Table 4). The results of both simplified and complex calculations also demonstrate comparatively larger optical section volumes in cats and dogs, ranging from 1.5- to 2.5-fold larger in comparison

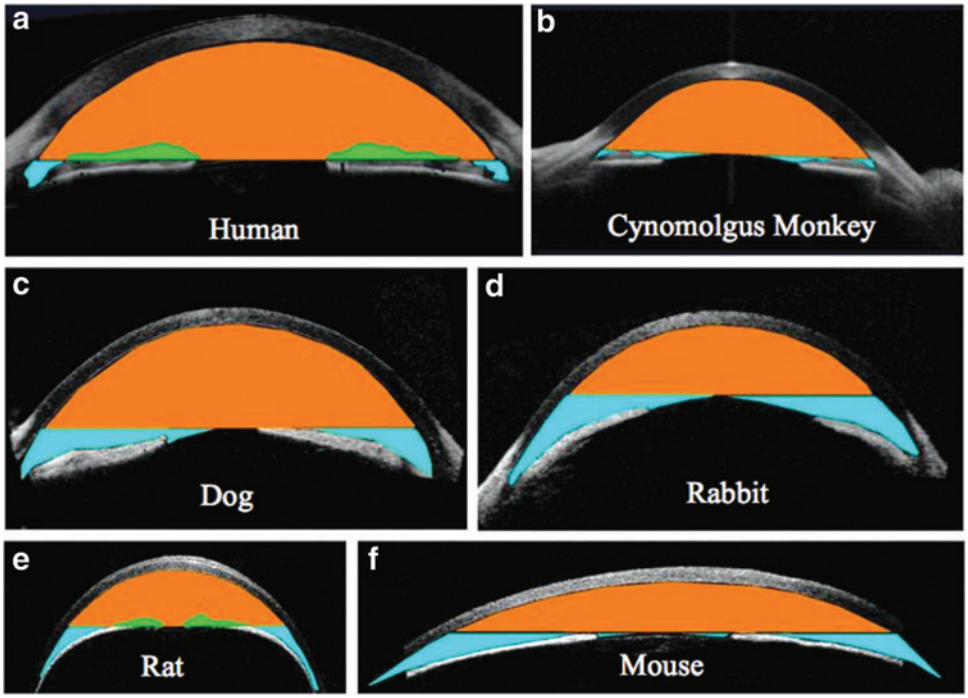

FIG. 2. A central anterior segment cross-section from a human **(a)**, cynomolgus monkey **(b)**, dog **(c)**, rabbit **(d)**, rat **(e)**, and mouse **(f)** using an image obtained by optical coherence tomography (OCT). The majority of the AC area is represented by *orange*, a reduction in AC area by iris is shown in *green*, and an increase in AC area is shown in *blue*. Note that the regions represented in *blue* and *green* result in a 4% decrease in the calculation of the human AC area and a 5% increase in the cynomolgus monkey AC area. Thus, anterior lens curvature has a minimal impact on calculation of AC volume in the human and cynomolgus monkey. However, the dog, rabbit, rat, and mouse would have significant underestimation of their AC volume if anterior lens curvature was not taken into account. Using the OCT images depicted here, the anterior lens curvature increased AC area in the dog, rabbit, rat, and mouse by 19%, 47%, 6% and 35%, respectively. Color images available online at www.liebertpub.com/jop

TABLE 4. COMPARISON OF THE VOLUME OF THE OPTICAL SECTION USED BY VARIOUS AC CELL GRADING SCHEMES

Species	*SUN (simplified)*[a] *(mm^3)*	*OSOD (simplified)*[a,b] *(mm^3)*	*OSOD (complex)*[b,c] *(mm^3)*	*OSOD–modified SUN (simplified)*[a] *(mm^3)*	*OSOD–modified SUN (complex)*[c] *(mm^3)*
Human	3.03	7.88	6.38	3.50	2.95
Cynomolgus	3.24	7.33	5.41	3.74	2.71
Cat	4.52	14.6	13.2	5.22	5.01
Dog	4.29	13.9	13.3	4.95	4.79
Rabbit	2.90	8.71	7.80	3.35	3.13
Pig	3.45	9.56	10.9	3.98	3.90
Rat	0.71	0.84	1.09	0.41	0.55
Mouse	0.45	0.33	0.25	0.16	0.13

[a]Calculation based on multiplication of beam area and AC depth with no adjustment for corneal curvature. This value is then multiplied by 1.15 to account for 30° light source.
[b]Calculation taking into account increased slit lamp height (14 mm). In species with a VCD less than the slit beam height used by OSOD, the VCD value is substituted for 14 mm.
[c]Calculation applying corneal curvature, with an increased volume to account for the 30° light source (varying from 5.3% to 10.2%, length modeled using a computer-aided drafting program), depending on the ratio of corneal curvature to AC depth. In species with a VCD less than the slit beam height used by OSOD (14 mm) or OSOD–modified SUN (10 mm), the VCD value is substituted for slit beam height.
VCD, vertical corneal diameter.

to humans, nonhuman primates, rabbits, and pigs. This difference is primarily due to a deeper AC in cats and dogs in comparison to all other species examined. Accordingly, the optical section volumes in these 2 species represent a smaller percentage of total AC volume for all 3 scoring systems examined (Table 5). In contrast, optical section volumes sampled using the SUN system are comparatively smaller in rats and mice, but represent a larger percentage of AC volume compared to all other species examined. This difference is primarily due to the relatively wide slit beam utilized in the SUN system.

Comparing the application of simplified and complex optical section volume calculations within a scoring system demonstrates the effect of species and features of anterior segment anatomy on AC cell density (cells/mm^3) (Table 6). In the human and cynomolgus monkey who share similar features of anterior segment anatomy, and thus, similar optical section volumes, the OSOD system provides relatively comparable AC cell density regardless of the calculation used. In smaller species like the rat and mouse, whose anterior segment geometry differs, however, AC cell counts determined using simplified formulae are considerably different from those determined with complex formulae. Compared to complex calculations, simplified calculations using the OSOD system may overestimate AC cell by as much as ~25% in the rat and may underestimate AC cell by ~30% in the mouse.

TABLE 5. COMPARISON OF THE OPTICAL SECTION VOLUME AS A PERCENTAGE OF AC VOLUME USING SLIT LAMP SPECIFICATIONS FOR VARIOUS AC CELL GRADING SCHEMES

Species	*SUN (simplified), %*	*OSOD (complex), %*	*OSOD–modified SUN (complex), %*
Human	1.8	3.8	1.8
Cynomolgus	3.2	5.4	2.7
Cat	0.6	1.6	0.6
Dog	0.6	1.8	0.6
Rabbit	1.0	2.8	1.1
Pig	1.3	4.2	1.5
Rat	4.6	7.3	3.6
Mouse	5.7	3.6	1.8

As SUN is widely considered the standard system for determining the AC cell in physician-based ophthalmology, use of the same system in preclinical investigations involving laboratory species would hypothetically improve translatability. Comparison of the application of both the SUN and the OSOD–modified SUN grading systems to optical volume calculations is presented in Table 7. The SUN system yields less variability in cell number per optical section volume in comparison to the OSOD–modified SUN and OSOD systems. It is noteworthy that this analysis utilized only a simplified calculation for the SUN system, as the dimensions of the beam would have yielded very similar values to the complex calculation. The observed differences between the 2 grading schemes are due to the dimension of the beam; the larger beam length used in the OSOD–modified SUN and OSOD systems is more susceptible to species differences in posterior corneal curvature and anterior lens curvature compared to the SUN system. Thus, use of the OSOD–modified SUN system results in dramatically different cell numbers per optical section volume between some species. While the OSOD–modified SUN grading scheme yields similar numbers of cells per optical section volume in humans, cynomolgus monkeys, and rabbits, this scheme yields lower cell counts per optical section volume, measuring ~75% of the values of the 3 aforementioned species in pigs and ~60% in dogs and cats. In addition, the smaller optical section volumes of mice and rats yield dramatically higher cell counts per optical section volume compared to larger species for both the SUN and OSOD–modified SUN systems. This analysis demonstrates the shortcomings of both systems in laboratory species and identifies the need for species-specific AC cell grading schemes for pigs, dogs, and cats, and for species with small eyes such as rats or mice, where cell numbers differ so significantly in comparison to larger animals.

Alternatively, the number of AC cells within the optical section can be standardized to human values for the SUN,

Table 6. Comparison of AC Cell Counts Per mm^3 of Optical Section Volume Using the OSOD AC Cell Grading Scheme

Species	*0*	*Trace/0.5+*	*1+*	*2+*	*3+*	*4+*
(A) OSOD simplified (AC cell/mm^3)						
Human	0	0–1	2–3	4–6	7–13	>13
Cynomolgus	0	0–1	2–3	4–7	8–14	>14
Cat	0	0–1	2	3	4–7	>7
Dog	0	0–1	2	3–4	5–7	>7
Rabbit	0	0–1	2–3	4–6	7–11	>11
Pig	0	0–1	2–3	4–5	6–10	>10
Rat	0	0–6	7–30	31–60	61–120	>120
Mouse	0	0–15	16–76	77–153	154–305	>305
(B) OSOD–complex (AC cell/mm^3)						
Human	0	0–1	2–4	5–8	9–16	>16
Cynomolgus	0	0–1	2–5	6–9	10–18	>18
Cat	0	0–1	2	3–4	5–8	>8
Dog	0	0–1	2	3–4	5–7	>7
Rabbit	0	0–1	2–3	4–6	7–13	>13
Pig	0	0–1	2	3–5	6–9	>9
Rat	0	1–5	6–23	24–46	47–92	>92
Mouse	0	0–20	21–99	100–198	199–397	>397

(A) Optical section volume using only the AC depth and light beam width and height (simplified), (B) optical section volume using the formulae described in Fig. 1 (complex). Note that the simplified calculations underestimate AC cell density by as much as 25%, 40%, 25%, 25%, and 15% in the human, cynomolgus monkey, cat, mouse, and rabbit, respectively, and also overestimate the AC cell density by as much as 50% and 30% in the pig and rat, respectively.

OSOD–modified SUN, and OSOD scoring schemes, respectively (Table 8). These modified scoring schemes can facilitate analysis in preclinical drug/device development programs by providing similar numeric scores across all species based on an equivalent number of cells per mm^3. In addition, conversion factors for each species were derived in the present study to facilitate direct comparison to humans for each scoring scheme in the event that data had been acquired in the past. Given the similarity of AC volume sampled, it is not surprising that cynomolgus monkeys and rabbits were the most similar to humans and required the smallest conversion factors in comparison to other species for all 3 scoring systems. However, conversion factors will be especially useful for species with substantially larger or smaller AC volumes sampled in comparison to humans, such as the cat, dog, and pig or rat and mouse, respectively, where up to a 50% adjustment is required depending on the grading scheme used.

Table 7. Number of AC Cells per mm^3 of Optical Section Volume

Species	*0*	*Trace (0.5+)*	*1+*	*2+*	*3+*	*4+*	*Percent of human value*
(A) SUN–simplified (AC cell/mm^3)							
Human	0	0–2	3–5	6–8	9–17	>17	100
Cynomolgus	0	0–2	3–5	6–8	9–16	>16	94
Cat	0	0–1	2–3	4–6	7–11	>11	67
Dog	0	0–1	2–4	5–6	7–12	>12	71
Rabbit	0	0–2	3–5	6–9	10–17	>17	104
Pig	0	0–1	2–4	5–7	8–15	>15	88
Rat	0	1–7	8–22	23–37	38–73	>73	442
Mouse	0	1–13	14–38	39–64	65–128	>128	772
(B) OSOD–modified SUN–complex (AC cell/mm^3)							
Human	0	0–2	3–5	6–9	10–18	>18	100
Cynomolgus	0	0–2	3–6	7–10	11–19	>19	107
Cat	0	0–1	2–3	4–5	6–11	>11	58
Dog	0	0–1	2–3	4–6	7–11	>11	61
Rabbit	0	0–2	3–5	6–9	7–17	>17	95
Pig	0	0–1	2–5	6–7	8–14	>14	77
Rat	0	1–10	8–30	31–50	51–101	>101	552
Mouse	0	1–44	45–131	132–219	220–437	>437	2,390

(A) The SUN and OSOD–modified SUN AC cell grading scheme; (B) optical section volume calculations derived using the formulae described in Fig. 1. A simplified calculation was used for the SUN system because the dimensions of the beam would yield very similar numbers to the complex calculation. For humans, cynomolgus monkeys, and rabbits, the SUN and OSOD–modified SUN grading schemes both yield similar cells per mm3 of optical section volume. However, both grading schemes result in cell counts per optical section volume measuring between 77%–88% of the human values in pigs, 58%–71% of the human values in dogs and cats, and 442%–2,390% in rats and mice.

Table 8. Number of AC Cells in Field for Each Species Using the SUN, OSOD–modified SUN, and OSOD Scoring Schemes

Species	*0*	*Trace (0.5+)*	*1+*	*2+*	*3+*	*4+*	*Conversion factor*
(A) SUN–simplified (AC cell in field)							
Human	0	1–5	6–15	16–25	26–50	>50	1.00
Cynomolgus	0	1–5	6–16	17–27	28–54	>54	0.94
Cat	0	1–8	9–23	24–38	39–75	>75	0.67
Dog	0	1–7	8–21	22–36	37–71	>71	0.71
Rabbit	0	1–5	6–14	15–24	25–48	>48	1.04
Pig	0	1–6	7–17	18–29	30–57	>57	0.88
Rat	0	0–1	2–3	4–5	6–12	>12	4.27
Mouse	0	<1	1–2	3	4–7	>7	6.73
(B) OSOD–modified SUN (complex) (AC cell in field)							
Human	0	1–5	6–15	16–25	26–50	>50	1.00
Cynomolgus	0	1–5	6–14	15–23	24–46	>46	1.09
Cat	0	1–9	10–26	27–43	44–85	>85	0.59
Dog	0	1–8	10–25	26–41	42–81	>81	0.62
Rabbit	0	1–5	6–16	17–27	28–53	>53	0.94
Pig	0	1–7	8–20	21–33	34–66	>66	0.76
Rat	0	<1	1–2	3–4	5–9	>9	5.37
Mouse	0	<1	<1	1	1–2	>2	22.7
(C) OSOD (complex) (AC cell in field)							
Human	0	1–5	6–25	26–50	51–100	>100	1.00
Cynomolgus	0	1–4	5–21	22–42	43–85	>85	1.18
Cat	0	2–10	12–52	53–104	105–207	>207	0.48
Dog	0	2–11	12–53	54–105	106–208	>208	0.48
Rabbit	0	1–6	7–31	32–61	62–122	>122	0.82
Pig	0	1–9	10–43	44–86	87–171	>171	0.58
Rat	0	<1	1–4	5–8	9–17	>17	5.84
Mouse	0	<1	1	2	3–4	>4	25.5

Data were calculated by multiplying the human values for AC cells per mm3 (from Tables 6B and 7A, B) by the optical section volumes for each species as shown in Table 5 for the SUN–simplified, OSOD–modified SUN complex, and OSOD–complex scoring schemes, respectively. A conversion factor for each species was determined by dividing the human AC cell in field by the AC cell in field for the species of interest. Cynomolgus monkeys and rabbits were the most similar to humans and required the smallest conversion factors in comparison to other species for all 3 scoring systems. Conversion factors will be especially useful for species with substantially larger AC volumes such as the cat, dog, and pig or species with substantially smaller AC volumes such as the rat or mouse in comparison to humans. The size of the conversion factor required for each grading scheme was SUN–simplified<OSOD–modified SUN complex<OSOD–complex.

The OCT images in Fig. 2 provide an *in vivo* illustration of comparative anterior segment anatomy and its effect on cross-sectional AC dimensions. In monkeys, for example, a larger radius of anterior lens curvature yields a demonstrably ''flatter'' anterior lens surface, therefore contributing only a minimal amount to the total AC volume. In contrast, the mouse, rat, dog, and rabbit have a smaller radius of curvature, which expands the effective AC volume. Using these images to quantify the additional chamber volume, AC area is increased by $\sim$20%–30% in the rabbit, mouse, and dog and to a lesser extent in the rat. Without considering this anatomical feature in these species, AC volume would be underestimated. The most accurate calculation of AC volume in a given species would consider additional anatomical features beyond those examined here. In some species, iris anatomy may also contribute to AC and optical section volumes. Represented in green in the OCT images in Fig. 2, iris volume visibly reduces the effective cross-sectional volume in the rat, but has little effect in other species. Iris location would also have a theoretical effect, but this feature would be more difficult to measure quantitatively, varying depending upon both the species and pupil diameter.

Veterinary ophthalmologists have observed both qualitative and quantitative differences in the ocular responses of certain laboratory species to identical insults (C.J. Murphy, P.E. Miller, pers. comm., 2014). For example, rabbits tend to exhibit a greater collective inflammatory response compared to nonhuman primates.[12] Nonhuman primates, however, tend to develop comparatively greater AC cell counts than rabbits, whose inflammatory responses are generally less cellular and characterized by greater degrees of aqueous flare. These differences may, in part, be a function of a species' ratio of uveal surface area to globe volume. In species with small eyes such as rats or mice, this ratio is considerably greater than in larger species and putatively translates into a comparatively greater capacity for these species to fill their ACs with inflammatory cells derived from the uvea.

The results demonstrated by this analysis take into consideration published or widely accepted species-specific anterior segment anatomy and geometry and, thus, provide a more accurate determination of optical section volume among common laboratory species. It should be acknowledged, however, that there is inherent uncertainty and variability to the reported values in Table 3, not only between different breeds and/or strains but also between individual animals. The effects of such variations are beyond the scope of this analysis, but may be an important subject of future investigation.

In conclusion, there are numerous factors to consider when choosing and interpreting a scoring system and grading scheme for AC cell. The SUN, OSOD–modified SUN, and OSOD scoring systems result in a similar number of cells per mm^3 of optical section in humans, cynomolgus monkeys, and rabbits. In comparison, all 3 grading schemes underestimate the number of cells per mm^3 in species with relatively larger AC volumes, such as pigs, dogs, and cats, as well as markedly overestimate the number of cells per mm^3 in species, such as rats and mice, with relatively smaller AC volumes in comparison to humans. The modified scoring schemes and conversion factors developed here yield more accurate AC cell densities per mm^3 across all species for the SUN, OSOD–modified SUN, and OSOD grading systems and, thus, will provide data that have a rational basis when comparing scores between species, and making interpretations with regard to number of cells per optical section volume sampled using a slit beam with defined dimensions.

Acknowledgments

This study was supported by Allergan and the National Institutes of Health K08 EY021142 and P30 EY12576, as well as an unrestricted grant from Research to Prevent Blindness to UC Davis. The authors thank Carol Rasmussen for providing the OCT images.

Author Disclosure Statement

No competing financial interests exist.

References

1. Jabs, D.A., Nussenblatt, R.B., Rosenbaum, J.T., et al. Standardization of uveitis nomenclature for reporting clinical data. Results of the First International Workshop. *Am. J. Ophthalmol.* 140:509–516, 2005.
2. Ghosn, C.R., Li, Y., Orilla, W.C., et al. Treatment of experimental anterior and intermediate uveitis by a dexamethasone intravitreal implant. *Invest. Ophthalmol. Vis. Sci.* 52:2917–2923, 2011.
3. Wiggans, K.T., Vernau, W., Lappin, M.R., et al. Diagnostic utility of aqueocentesis and aqueous humor analysis in dogs and cats with anterior uveitis. *Vet. Ophthalmol.* 17:212–220, 2014.
4. Donnelly, J.J., Taylor, H., Young, E., et al. Experimental ocular onchocerciasis in cynomolgus monkeys. *Invest. Ophthalmol. Vis. Sci.* 27:492–499, 1986.
5. Gilger, B.C., Abarca, E.M., Salmon, J.H., et al. Treatment of acute posterior uveitis in a porcine model by injection of triamcinolone acetonide into the suprachoroidal space using microneedles. *Invest. Ophthalmol. Vis. Sci.* 54:2483–2492, 2013.
6. Eom, Y., Lee, D.Y., Kang, B.R., et al. Comparison of aqueous levels of inflammatory mediators between toxic anterior segment syndrome and endotoxin-induced uveitis animal models. *Invest. Ophthalmol. Vis. Sci.* 55:6704–6710, 2014.
7. Wang, J., Lu, H., Hu, X., et al. Nuclear factor translocation and acute anterior uveitis. *Mol. Vis.* 17:170, 2011.
8. Munger, R.J. Veterinary ophthalmology in laboratory animal studies. *Vet. Ophthalmol.* 5:167–175, 2002.
9. Attar, M., Brassard, J.A., Kim, A.S., et al. Safety evaluation of ocular drugs. In: Faqi, A.S., ed. *A Comprehensive Guide to Toxicology in Preclinical Drug Development.* San Diego: Academic Press; 2013.
10. Kass, M., Palmberg, P., and Becker, B. The ocular anti-inflammatory action of imidazole. *Invest. Ophthalmol. Vis. Sci.* 16:66–69, 1977.
11. Krzystolik, M.G., Afshari, M.A., Adamis, A.P., et al. Prevention of experimental choroidal neovascularization with intravitreal anti-vascular endothelial growth factor antibody fragment. *Arch. Ophthalmol.* 120:338–346, 2002.
12. Stern, F., and Bito, L. Comparison of the hypotensive and other ocular effects of prostaglandins E2 and F2 alpha on cat and rhesus monkey eyes. *Invest. Ophthalmol. Vis. Sci.* 22:588–598, 1982.
13. Jonas, J.B., Holbach, L., and Panda-Jonas, S. Scleral cross section area and volume and axial length. *PLoS One.* 9:e93551, 2014.
14. Augusteyn, R.C., Nankivil, D., Mohamed, A., et al. Human ocular biometry. *Exp. Eye Res.* 102:70–75, 2012.
15. Navarro, R., Santamaría, J., and Bescós, J. Accommodation-dependent model of the human eye with aspherics. *J. Opt. Soc. Am. A.* 2:1273–1280, 1985.
16. O'Donnell, C., Hartwig, A., and Radhakrishnan, H. Comparison of central corneal thickness and anterior chamber depth measured using LenStar LS900, Pentacam, and Visante AS-OCT. *Cornea.* 31:983–988, 2012.
17. Wang, D., Qi, M., He, M., et al. Ethnic difference of the anterior chamber area and volume and its association with angle width. *Invest. Ophthalmol. Vis. Sci.* 53:3139–3144, 2012.
18. Manns, F., Fernandez, V., Zipper, S., et al. Radius of curvature and asphericity of the anterior and posterior surface of human cadaver crystalline lenses. *Exp. Eye Res.* 78:39–51, 2004.
19. Assia, E.I., and Apple, D.J. Side-view analysis of the lens: I. The crystalline lens and the evacuated bag. *Arch. Ophthalmol.* 110:89–93, 1992.
20. Lapuerta, P., and Schein, S.J. A four-surface schematic eye of macaque monkey obtained by an optical method. *Vision Res.* 35:2245–2254, 1995.
21. Kaufman, P.L, Calkins, B.T, Erickson, K.A. Ocular biometry of the cynomolgus monkey. *Curr. Eye Res.* 1:307–309, 1981.
22. Greenbaum, S., Lee, P.Y., Howard-Williams, J., et al. The optically determined corneal and anterior chamber volumes of the cynomolgus monkey. *Curr. Eye Res.* 4:187–190, 1985.
23. Nankivil, D., Manns, F., Arrieta-Quintero, E., et al. Effect of anterior zonule transection on the change in lens diameter and power in cynomolgus monkeys during simulated accommodation. *Invest. Ophthalmol. Vis. Sci.* 50:4017–4021, 2009.
24. Vakkur, G., and Bishop, P. The schematic eye in the cat. *Vision Res.* 3:357–381, 1963.
25. Carrington, S.D., and Woodward, E.G. Corneal thickness and diameter in the domestic cat. *Ophthalmic Physiol. Opt.* 6:385–389, 1986.
26. Rankin, A.J., Crumley, W.R., and Allbaugh, R.A. Effects of ocular administration of ophthalmic 2% dorzolamide hydrochloride solution on aqueous humor flow rate and intraocular pressure in clinically normal cats. *Am. J. Vet. Res.* 73:1074–1078, 2012.
27. Samuelson, D.A. Ophthalmic anatomy. In: Gelatt, K.N., Gilger, B.C., Kern, T.J., eds. *Veterinary Ophthalmology.* New Jersey: Wiley; 2013; p. 39–170.
28. Mutti, D.O., Zadnik, K., and Murphy, C.J. Naturally occurring vitreous chamber-based myopia in the Labrador retriever. *Invest. Ophthalmol. Vis. Sci.* 40:1577–1584, 1999.

29. Coile, D., and O'Keefe, L. Schematic eyes for domestic animals. *Ophthalmic Physiol. Opt.* 8:215–219, 1988.
30. Gilger, B.C., Reeves, K.A., and Salmon, J.H. Ocular parameters related to drug delivery in the canine and equine eye: aqueous and vitreous humor volume and scleral surface area and thickness. *Vet. Ophthalmol.* 8:265–269, 2005.
31. Bozkir, G., Bozkir, M., Dogan, H., et al. Measurements of axial length and radius of corneal curvature in the rabbit eye. *Acta Med. Okayama.* 51:9–11, 1997.
32. Tsonis, P.A. *Animal Models in Eye Research.* San Diego: Academic Press; 2008.
33. Wong, K., Koopmans, S.A., Terwee, T., et al. Changes in spherical aberration after lens refilling with a silicone oil. *Invest. Ophthalmol. Vis. Sci.* 48:1261–1267, 2007.
34. Sanchez, I., Martin, R., Ussa, F., et al. The parameters of the porcine eyeball. *Graefes Arch. Clin. Exp. Ophthalmol.* 249:475–482, 2011.
35. Johnson, M., Caro, N., and Huang, J.D. Adequacy of exchanging the content of the anterior chamber. *Exp. Eye Res.* 91:876–880, 2010.
36. Vilupuru, A.S., and Glasser, A. Optical and biometric relationships of the isolated pig crystalline lens. *Ophthalmic Physiol. Opt.* 21:296–311, 2001.
37. Massof, R.W., and Chang, F.W. A revision of the rat schematic eye. *Vision Res.* 12:793–796, 1972.
38. Bawa, G., Tkatchenko, T.V., Avrutsky, I., et al. Variational analysis of the mouse and rat eye optical parameters. *Biomed. Opt. Express.* 4:2585–2595, 2013.
39. Mermoud, A., Baerveldt, G., Minckler, D.S., et al. Aqueous humor dynamics in rats. *Graefes Arch. Clin. Exp. Ophthalmol.* 234:S198-S203, 1996.
40. Pe'er, J., Muckarem, M., and Zajicek, G. Epithelial cell migration in the normal rat lens. *Ann. Anat.* 178:433–436, 1996.
41. Remtulla, S., and Hallett, P. A schematic eye for the mouse, and comparisons with the rat. *Vision Res.* 25:21–31, 1985.
42. Zhang, D., Vetrivel, L., Verkman, A. Aquaporin deletion in mice reduces intraocular pressure and aqueous fluid production. *J. Gen. Physiol.* 119:561–569, 2002.
43. Mailankot, M., Staniszewska, M.M., Butler, H., et al. Indoleamine 2, 3-dioxygenase overexpression causes kynureninemodification of proteins, fiber cell apoptosis and cataract formation in the mouse lens. *Lab. Invest.* 89:498–512, 2009.

Received: June 19, 2015
Accepted: October 5, 2015

Address correspondence to:
Dr. Sara M. Thomasy
Department of Surgical and Radiological Sciences
School of Veterinary Medicine
University of California, Davis
One Shields Avenue
Davis, CA 95616

E-mail: smthomasy@ucdavis.edu